The surface reactivity and implied toxicity of ash produced from sugarcane burning

THE SURFACE REACTIVITY AND IMPLIED TOXICITY OF ASH PRODUCED FROM SUGARCANE BURNING

Jennifer S Le Blond[†,‡]*, Maura Tomatis[§,‖]^, Claire J Horwell[#], Christina Dunster[††], Fiona Murphy[‡‡], Ingrid Corazzari[§,‖], Francesca Grendene[§,‖], Francesco Turci[§,‖], Elena Gazzano[‖,§§], Dario Ghigo[‖,§§], Ben J. Williamson[‖‖], Clive Oppenheimer[†,##,†††], Bice Fubini[§,‖]

[†]Department of Geography, University of Cambridge, Downing Place, Cambridge, CB2 3EN, UK.

[‡]Department of Mineralogy, Natural History Museum, Cromwell Road, London, SW7 5BD, UK.

[§]Dipartimento di Chimica I.F.M., Università degli studi di Torino Via P. Giuria 7, 10125, Torino, Italy.

[‖]"G. Scansetti" Interdepartmental Center for Studies on Asbestos and other Toxic Particulates, Università degli studi di Torino, Via P. Giuria 7, 10125, Torino, Italy.

[#]Institute of Hazard, Risk and Resilience, Department of Earth Sciences, Durham University, Science Labs, South Road, Durham, DH1 3LE, UK.

[††]Lung Biology Group, Pharmaceutical Science Division, King's College London, SE1 9NH, UK.

[‡‡]MRC Centre for Inflammation Research, The Queen's medical Research Institute, 47 Little France Crescent, Edinburgh EH16 4TJ, UK.

[§§]Dipartimento di Genetica, Biologia e Biochimica, Università degli studi di Torino, Via Santena, 5/bis, 10126, Torino, Italy.

[‖‖]Camborne School of Mines, College of Engineering, Mathematics and Physical Sciences, University of Exeter, Penryn, Cornwall TR10 9EZ, UK.

[##]Le Studium, Institute for Advanced Studies, Orléans and Tours, France.

[†††]Istitut des Sciences de la Terre d'Orléans, 1a rue de la Férollerie, 45071 Orléans, Cedex 2, France.

***CORRESPONDING AUTHOR (1):** Dr Jennifer S Le Blond

Address: Department of Mineralogy, Natural History Museum, Cromwell Road, London, SW7 5BD, UK

Tel: +44 (0) 7850 307228

Fax: +44 (0) 20 7942 5537

Email: jennl3@nhm.ac.uk

^**CORRESPONDING AUTHOR (2):** Dr Maura Tomatis

Address: "G. Scansetti" Interdepartmental Center for Studies on Asbestos and other Toxic Particulates, Università degli studi di Torino, Via P. Giuria 7, 10125, Torino, Italy.

Ph. +39 011 670.7577

Fax +39 011 670.7577

Email: m.tomatis@unito.it

ABSTRACT

Sugarcane combustion generates fine grained particulate which has the potential to be a respiratory health hazard because of its grain size and composition. In particular, conversion of amorphous silica to crystalline forms during burning may provide a source of toxic particles. In this study we investigate and evaluate the toxicity of sugarcane ash and bagasse ash formed from commercial sugarcane burning. Experiments to determine the main physico-chemical properties of the particles, known to modulate biological responses, were combined with cellular toxicity assays to gain insight into the potential reactions that could occur at the particle-lung interface following inhalation.

The specific surface area of the particles ranges from ~16 to 90 m^2 g^{-1}. The samples did not generate hydroxyl or carbon-centred radicals in cell-free tests. However, all samples wereable to 'scavenge' an external source of hydroxyl radicals, which may be indicative of defects on the particle surfaces that may interfere with cellular processes. The bio-available iron on the particle surfaces was low (2-3 µmol m^{-2}) indicating a low propensity for iron-catalysed radical generation. The sample surfaces were all hydrophilic and slightly acidic, which may be due to the presence of oxygenated (functional) groups. The ability to cause oxidative stress and membrane rupture in red blood cells (haemolysis) was found to be low, indicating that the samples are not toxic by the mechanisms tested. Cytotoxicity of sugarcane ash was observed, by measuring lactate dehydrogenase release, after incubation of relatively high concentrations of ash with murine alveolar macrophage cells. All samples induced nitrogen oxide release (although only at very high concentrations) and reactive oxygen species generation (although the bagasse samples were less potent than the sugarcane ash). However, the samples induced significantly lower cytotoxic effects and nitrogen oxide generation, when compared with the positive control.

KEY WORDS: sugarcane ash, particulate, toxicity, health hazard

INTRODUCTION

Commercial sugarcane crops are routinely burned before they are harvested to remove superfluous leaf (trash) material, principally to increase cutting efficiency. Epidemiological investigations have linked commercial pre- and post- harvest sugarcane burning with detrimental health in local populations (Ribeiro, 2009; Cançado et al., 2006), especially with an increase in respiratory diseases (Arbex et al., 2007; Lopes and Ribeiro, 2006) such as asthma (Boopathy et al., 2002; Arbex et al., 2000) and heightened risk of lung cancer (Amre et al., 1999).

Toxicology studies on sugarcane combustion products are rare. Mazzoli-Rocha et al., (2008) determined that a single, low dose of particles collected from pre-harvest sugarcane burning can induce significant alterations in the pulmonary mechanism in mice and determined that the overall impact was at least as toxic as traffic-derived particles. Previous studies characterising sugarcane combustion products show that amorphous silica, present in the stems and leaves of sugarcane, can convert to crystalline silica during combustion (Le Blond et al., 2010; 2008). Cristobalite, a high temperature polymorph of crystalline silica, is a certified human lung carcinogen (IARC, 1997). Sugarcane ash also contains abundant carbon and it is known that inhalation of carbon-rich dust can cause the formation of localised nodules within the lung, containing macrophage cells burdened with carbonaceous particles (e.g. Fubini and Otero Areán, 1999). Although carbon particles do not cause cell death (lysis) in the same way as crystalline silica particles, heavy and prolonged exposure can impair lung function.

In this paper, we investigate whether the airborne particulate (i.e. an air-suspended mixture of solid and liquid particles that vary in size, shape and composition, e.g. Pope III, 2000), released during sugarcane burning, could be a factor in the poor health of workers and surrounding populations. Inhaled particles primarily interact with the lung lining layer containing surfactants, proteins and other organic molecules, some of which (e.g. glutathione and ascorbic acid) are

involved in the antioxidant defences. Depending on particulate aerodynamic diameter, the ash may reach the alveoli in the deep lung, where particles may be engulfed by alveolar macrophages (AM), and be successfully removed from the lung. If this process fails, macrophages become activated and release transcription factors, reactive oxygen species (ROS) and reactive nitrogen species (RNS), cytokines, chemotactic and growth factors etc., which result in eventual cell death, and (re-)release of the engulfed particles into the alveolar space. A continuous cycle of recruitment and cell death may become established, causing sustained inflammation (as long as the particle resides in the lung), which results in damage to the surrounding epithelial cells and stimulates abnormal fibroblast growth.

The molecular mechanisms implied in particle toxicity, thus, appear complex. Nevertheless, specific physico–chemical features (Fubini and Otero-Areán, 1999; Hardy and Aust, 1995) and cellular responses (Jaurand, 1997) can be related to a dust's level of toxicity and can be used as markers to estimate the likely toxic reaction in newly-studied materials.

In the case of sugarcane burning, particulate is formed in several ways. In addition to the smoke generated during the burn itself, ash deposits are also formed and are the focus of this paper as they encompass the bulk of occupational exposure. Bagasse is formed after the sugarcane stalks have been crushed during sucrose extraction and is commonly burned in the processing factory to supply energy for the sugar-production process, generating bagasse ash in the process. Sugarcane ash is the product remaining in the field following a burn and can be easily broken down into a respirable size by mechanical disturbance.

The following paper evaluates the toxicity of sugarcane and bagasse ash by a) determining the dusts' physico-chemical properties considered relevant to their toxicity, including: particle size, shape and surface area, surface reactivity (namely potential for free radical generation, iron

release, depletion of endogenous antioxidants, surface charge and degree of hydrophilicity/hydrophobicity), and b) assessment of the reaction during four standard toxicity assays: haemolysis (red blood cell membrane rupture, i.e. death), cytotoxicity, ROS and nitric oxide (NO) generation in murine alveolar macrophages. The following study represents a model approach to the general problem of estimating the potential toxic reaction in samples where exposure information and in vivo experimental data are not readily available.

Particle surface reactivity

Among all possible reactions, free radical generation is most strongly implicated in the mechanisms of particulate respiratory toxicity. When in contact with biological fluids many mineral particulate (dust) samples generate free radicals via various mechanisms (Schoonen et al., 2006; Fubini and Hubbard, 2003). Two radical-generating mechanisms are investigated here: a) Hydroxyl radical ($HO^{\bullet}$) generation through the Fenton reaction, an iron-catalysed reaction in the presence of hydrogen peroxide (H_2O_2), which mimics contact of the particles with H_2O_2 produced by cell-generated superoxide anions. Iron-induced free radical generation has been shown to cause lung inflammation and carcinogenesis (Kane, 1996; Hardy and Aust, 1995), and b) Carboxylate radicals ($CO_2^{-\bullet}$) from the formate ion, used as a model target molecule for homolytic cleavage of a carbon-hydrogen bond. In addition, we also investigate whether the ash acts as 'scavengers' of preformed oxygen-centred free radicals which may be indicative of defects on the particle surfaces that may interfere with cellular processes.

The surface charge and hydrophilicity of the surface will influence whether particles within the sample will be easily dispersed or tend to agglomerate into larger (i.e. non-respirable) sizes, and give an indication of their propensity to interact with cell membranes (i.e. adsorb phospholipids and proteins; Miller et al., 1998; Van Oss, 1994; Light and Wei, 1977).

The potential for inhaled particles to provoke oxidative injury at the lung-air boundary is primarily controlled by the reaction of the antioxidant defenses (pro-oxidant and pro-inflammatory responses; Ayres et al., 2008). The strength of an individual's antioxidant defenses is also an important consideration, as asthma sufferers can have an enhanced sensitivity to air pollutants, due to their impaired antioxidant defenses (Li et al., 2003; Kelly et al., 1999). The oxidative potential of particles can be quantified by monitoring the depletion of the antioxidant during incubation with ascorbate over time (Ayres et al., 2008).

Cellular assays

Red blood cells (erythrocytes) transport oxygen in the blood and are at risk of oxidation injury from endogenous substances (e.g. H_2O_2, produced in response to inflammation) or exogenous chemicals. Erythrocyte lysis (haemolysis) is a relatively simple and inexpensive test commonly used to monitor whether a mineral dust sample can cause cell rupture (lysis) when incubated with erythrocytes in a quartz-like response.

The capacity for some toxic particles to produce ROS and NO, has been associated with cytotoxic and mutagenic effects (Park and Aust, 1998), and can be investigated by assessing the leakage of lactate dehydrogenase (LDH) from murine alveolar macrophages (MH-S). The loss of LDH from MH-S cells into the culture medium is an indicator of cell membrane damage. In macrophages NO is primarily produced by the inducible NO synthase (iNOS) isoform, and plays an important role in non-specific immune responses (Schmidt and Walter, 1994). During a chronic inflammatory reaction, however, the levels of NO are elevated above normal levels within the tissues, which can be toxic for host cells. NO can react with superoxide anions ($O_2^{\bullet -}$), to produce

peroxynitrite ($ONOO^-$) that can generate $HO^\bullet$ radicals and RNS, which are able to interact with proteins and nucleic acids (Wink and Mitchell, 1998).

MATERIALS AND METHODS

Samples of ash were collected from two commercial sugarcane-growing estates in different South American countries (including Brazil; Table 1). The species of sugarcane grown at each of the estates was the same (Saccharum officinarum), although they differed in genetic variety. Five burning events were sampled in Country A and two in Country B (confidentiality agreed with the sugarcane estates). The area of plot burned varied from 12-17 ha. All samples were kept in dry storage until analysis. All samples contain silica (between approximately 10 and 25 wt. % SiO_2, in the sugarcane ash and up to 40 % in the bagasse ash, mostly in an amorphous form, but with a small amount of quartz, up to 3.5 wt. %), C, Al, Fe, Mg, and K in variable amounts (Le Blond et al., 2010).

TABLE 1

All experiments were carried out at the Università degli studi di Torino, Italy, unless stated.

Particle surface area, size and shape

Specific surface area analysis was carried out by BET nitrogen absorption on a Micromeritics Gemini analyser at the Natural History Museum, London, UK. Prior to analysis, all samples were degassed under a continuous N_2 flow at 100 $^{\circ}$C for at least 12 hr (e.g. Greg and Sing, 1982). Each sample was analysed at least 3 times and averaged.

Characterization of the respirable fraction, in two samples (A_ash1 and A_ashbag1), were carried out using the Sysmex FPIA-3000 Flow Particle Image Analyzer (Malvern Instruments), which enables measurement of particle number as well as particle size and shape. A <5 μm diameter fraction of particulate was isolated by sedimentation in isopropanol, and a diluted (0.5 mg ml^{-1})

suspension was passed through a cell where stroboscopic illumination and a CCD camera lens (at 20 times magnification) captured images of the particles, and the minor and major axis (i.e. width and length) of the individual particles were measured The suspension was sonicated for 30 s at ~10 watt, before image analysis, to encourage disaggregation of the particles.

Particle surface reactivity

Free radical production

The spin trap technique, combined with electron paramagnetic resonance (EPR), can be used to detect free radicals released from the sample surface (Fubini et al., 1995a; Shi et al., 1995; Fubini et al., 1990; Giamello et al., 1990; Dalal et al., 1990). Free radical species have a short half life (~0.001 s), however, they can be stabilized by the spin trap agent DMPO (5,5'-dimethyl-1-pyrroline-N-oxide), thereby facilitating measurement by EPR. The production of $CO_2^{\bullet-}$ radicals was measured with and without ascorbic acid, which reduces Fe^{3+} to Fe^{2+} and promotes cleavage of the C-H bond. $HO^{\bullet}$ generation was measured by suspending 150 mg of ash in 500 µl of 0.5 M phosphate-buffered solution (pH 7.4), then adding 250 µl of 0.17 M DMPO and 500 µl of 0.2 M H_2O_2. For the measurement of $CO_2^{\bullet-}$ radicals, 500 µl of 0.17 M DMPO was added to 150 mg of ash, after which 500 µl of a solution of 2 M sodium formate in 0.5 M phosphate buffer was also added. In half of the experiments, 1.5 mM ascorbic acid was added to the sodium formate in phosphate buffer solution (purchased from Alexis, Lausen, Switzerland). All other reagents were purchased from Sigma-Aldrich S.r.l. (Milan, Italy). The results are expressed per unit surface area.

All experiments included ash-free control solutions and all suspensions were stirred for 1 hr in a darkened vial. Aliquots of the suspension were withdrawn after 10, 30 and 60 min and filtered through cellulose acetate (0.20 µm porosity) filters. The liquid was introduced into a 50 µL

capillary tube and placed in a Miniscope 100 ESR spectrometer (Magnettech), using the following parameters: microwave power 10 mW, modulation amplitude 1 G, scan time 80 s, number of scans 2. Each sample was tested at least twice. The amount of free radicals produced was quantified by integrating the amplitude of the peaks generated in each spectrum.

The potential $HO^{\bullet}$ scavenging activity of the ash samples was investigated using a similar technique to that outlined in Fenoglio et al., (2008). For this, substantial amounts of $HO^{\bullet}$ were generated (via the Fenton reaction) by adding 250 µl of 0.2 M H_2O_2 to a solution of 250 µl of 0.5 M phosphate buffer (pH 7.4), 125 µl of 0.17 M DMPO and 100 µl of 13 mM $FeSO_4$. This reaction was repeated in the presence of a suspension of 75 mg of the sample. The intensity of the EPR spectrum (of the DMPO/$HO^{\bullet}$ adducts) was measured, in the same way as above.

Bio-available Iron

The amount of bio-available iron on the sample surface can be evaluated by mobilization of ferric and ferrous ions using specific chelators. The amount of reduced iron was measured using ferrozine, a bidentate N donor chelator (pH 4) specific for Fe^{2+}. Ascorbic acid was used in half of the experiments (to reduce Fe^{3+} to Fe^{2+}) to measure the total amount of Fe (i.e. Fe^{3+} + Fe^{2+}) mobilized (Horwell et al., 2007; 2003; Hardy and Aust 1995).

Four ash samples (~20 mg) were placed in tubes with 20 mL of 1 mM solutions of just ferrozine or ferrozine plus ascorbic acid (1 mM). Three repeats of each sample were prepared. The suspensions were continuously stirred at 37 $^{\circ}$C. After 24 hr the samples were removed, centrifuged for 30 min and an aliquot of the supernatant was analysed. The ferrozine forms a coloured complex with Fe^{2+} and the intensity of the colour change was measured in a Uvikon 930 dual beam spectrophotometer (Kontron Instrument; 562 nm, E_{mM} = 27.9 mM^{-1} cm^{-1}). The samples were then returned to the incubator and measured in this way every 24 hr for 7 days. Two control

252 solutions, of ferrozine with deionised water and ferrozine with ascorbic acid, showed no colour
253 change over the experiment. The results are expressed per unit surface area.
254
255 *Depletion of endogenous antioxidants*
256 The oxidative potential of particles was quantified by monitoring the depletion of the antioxidant
257 during incubation with ascorbate over time. A known weight of each of the ash samples was re-
258 suspended in 5 % methanol/95 % chelex-treated water at pH 7.0 at 150 µg mL^{-1}, sonicated and an
259 aliquot diluted to 12.5 µg mL^{-1}. Triplicate aliquots were incubated for 10 min at 37 $^{\circ}$C in a 96
260 multiwell plate, followed by the addition of a final concentration of 200 µM ascorbate solution.
261 The experiments included a number of controls; M120 (negative control, model carbon black
262 sample; e.g., Godri et al., 2010), ROFA (positive control, which contains ~10 wt. % water soluble
263 Fe, Ni and V; Kelly, 2003) LEZ B11-14 (airborne particulate matter collected in London:
264 medium oxidation response) and LEZ 11-20 (airborne particulate collected in London: low
265 oxidation response), which were run simultaneously. All samples were run at a final
266 concentration of 10 µg mL^{-1}. A Spectramax 190 plate reader (Molecular Devices at the Lung
267 Biology Group, King's College London, UK) set to 265 nm, 37 $^{\circ}$C with associated SoftMaxPro
268 software was used to record the decrease in ascorbic acid absorbance every 2 min and monitored
269 for a total of 2 hr.
270
271 Each of the samples was also run with the addition of 200 µmol L^{-1} of DTPA (diethylene triamine
272 pentaacetic acid). DTPA is a chelating agent which is used to sequester any transition metal
273 cations that may be present in the ash samples. The oxidation potential of this solution is also
274 monitored and would indicate the contribution of transition metal ions, if present, to the overall
275 oxidative potential of the sample.
276
277 *Surface hydrophilicity*

The degree of surface hydrophilicity was tested by measuring the interaction of sample ash surfaces with water vapour using adsorption micro-calorimetry (Fubini et al., 1989). The samples were outgassed in calorimetric cells overnight at 150 °C to remove any molecularly-adsorbed water without affecting the surface hydroxyl population (Bolis et al., 1985). The heat of water adsorption onto the sample surface was measured by a Tian-Calvet micro-calorimeter (Setram) which was connected to volumetric apparatus. This allowed simultaneous measurement of the quantity of adsorbed water, heat released and equilibrium pressure after small amounts of water vapour were allowed to interact with the sample. The pressure of the system was monitored with a 0-100 torr (1 torr = 133.322 Pa) transducer gauge (Baratron MKS) and the temperature of the calorimeter was maintained at ~25 °C.

A typical adsorption sequence comprised three runs; (i) dosing successive amounts of water vapour onto the sample up to a defined equilibrium pressure, typically 10 Torr (Adsorption I), (ii) desorption at 30 °C under vacuum, and (iii) re-adsorption of similar doses up to the same equilibrium pressure, in order to evaluate the fraction of adsorbate which is reversibly held at the surface (Adsorption II). The adsorption sequence is not replicated and no standard deviation is calculated, as the equilibrium pressure may vary slightly between experiments.

Particle surface charge

The surface charge of the sample was evaluated by measuring the zeta potential using a NanoZetaSizer System (Malvern Instruments). The pH of the ash suspensions (0.3 % in distilled water) was adjusted (between pH 2.0 and 8.0) with dilute acid (HCl) or base (NaOH) solutions and then the suspension was allowed to stand for 15 min in order to let the larger particles settle.

Cellular assays

Erythrocyte lysis (haemolysis)

*T*he erythrocyte lysis test was carried out at the Centre for Inflammation Research, University of Edinburgh, UK, following a similar method to Clouter et al., (2001). Erythrocytes were obtained from fresh human venous blood and the washed erythrocytes were incubated with TiO_2 (negative control), DQ12 quartz (a highly positive control known to cause cell lysis), and the ash samples for a period of 20 min. The subsequent % haemolysis was determined by measuring the absorbance at 550 nm. All particles were probe sonicated for 5 min prior to use in the assay.

Murine alveolar macrophages (MH-S) cellular response

MH-S cells (provided by Istituto Zooprofilattico Sperimentale "Bruno Ubertini", Brescia, Italy), were cultured in 35 mm diameter Petri dishes in RPMI-1640 medium (Gibco, Paisley, UK) supplemented with 10 % foetal bovine serum (FBS) at up to 90 % confluence. In each of the three experiments, 0, 20, 40, 80, 120 μg cm^{-2} concentrations of ash sample were added to the culture medium and incubated for 24 hr. Min-U-Sil 5 quartz (crystalline, US Silica Company, Berkeley Springs, WV), the most widely employed silica sample in in vitro and in vivo studies (IARC, 1997), was used as a positive control because of its high cytoxicity and high potential to generate ROS and RNS. The protein content of the cell monolayers, cell suspensions and cell lysates was assessed with the bicinchoninic acid protein assay (BCA) kit. The results were analyzed by a one-way Analysis of Variance (ANOVA) and Tukey's test and $p < 0.05$ was considered significant.

Extracellular LDH activity

The cytotoxic effect of two samples of ash were measured as leakage of lactate dehydrogenase (LDH) activity into the extracellular medium, as previously described (Polimeni et al., 2008). Briefly, after 24 hr incubation with the sample, at varying concentrations (as above), the extracellular medium was collected and centrifuged at 13,000 x g for 30 min. The cells were washed with fresh medium, detached with trypsin/ethylenediaminetetraacetic acid (EDTA, a

chelating agent; 0.05/0.02 % v/v), washed with a phosphate-buffer solution (PBS), re-suspended in 1 ml of TRAP (triethanolamine 82.3 mM, pH 7.6), and sonicated on ice with two 10 s bursts. LDH activity was measured in the extracellular medium and in the cell lysate (solution produced during cell lysis), using a Synergy HT microplate reader (Biotek Instruments, Winooski, VT). Both intracellular and extracellular enzyme activity was expressed as µmol of NADH oxidized/min/dish, then extracellular LDH activity (LDH out) was calculated as percentage of the total (intracellular + extracellular) LDH activity (LDH tot) in the dish.

Nitric oxide (NO) synthesis

After a 24 hr incubation with control and the above reported concentrations of ash samples, the extracellular medium was removed and the extracellular nitrite level (a stable derivative of NO) was measured using the Griess method as previously described (Ghigo et al., 1998). Nitrite was measured at 540 nm with a Synergy HT microplate reader. A blank was prepared in the absence of cells and its absorbance was subtracted from that measured in the samples; absorbance values were also corrected for (considering monolayer proteins) and results were expressed as nmol mg^{-1} cellular protein.

Reactive oxygen species (ROS)

After a 24 hr incubation in the absence or presence of the samples of ash (at different concentrations, as above), MH-S cells were loaded for 15 min with 10 µM 2',7'-dichlorodihydrofluorescein diacetate (DCFH-DA). DCFH-DA is a cell-permeable probe that is cleaved intracellularly by (nonspecific) esterases to form DCFH, which is further oxidized by ROS to form the fluorescent compound dichlorofluorescein (DCF). After 24 hr incubation with the samples and control, the cells were washed twice with PBS and the DCF fluorescence was determined at an excitation wavelength of 504 nm and emission wavelength of 529 nm, using a

Perkin-Elmer LS-5 fluorimeter (Perkin Elmer, Shelton, CT). The fluorescence value was normalized by protein concentration and expressed as μmol mg^{-1} cellular protein.

Table 2 indicates the selected analysis performed on each of the sugarcane and bagasse ash samples.

TABLE 2

RESULTS

Particle surface area, size and shape

Sample surface area varied between ~16 to 90 $m^2 g^{-1}$ (Table 3), with an average of 55.8 $m^2 g^{-1}$ for sugarcane ash and 59.0 $m^2 g^{-1}$ for the bagasse ash. The majority of the ash samples analysed by nitrogen absorption yielded a strongly negative BET-fit intercept (C-value), which is assumed to give an indication of the sample to gas interaction energy (Sing et al., 1985). A negative C-value is an indication that there is weak interaction between the nitrogen and sample, and so the BET model (i.e. multilayer absorption) is a poor fit (e.g. Baker et al., 2004). In these situations, the Langmuir surface area, which represents a monolayer adsorption of nitrogen molecules, is taken instead of the BET surface area value.

TABLE 3

Ash samples were very heterogeneous both in size and morphology. Despite the high surface area, the mean diameter of the particles ranged from 46 to 176 µm (Table 3). The sub-5 µm fraction particles, imaged in the Flow Particle Image Analyser, ranged from elongated in morphology to spherical or spheroid-shaped with smooth surfaces (i.e. the aspect ratio had a wide spread, Fig. 1a and b) and very few aggregates were observed in the images. The sample of sugarcane ash was generally finer than the bagasse ash. Both samples contained some acicular and fibre-like (length to width ratio >3:1) particles (Fig. 1c and d). The fibre-like particles were more abundant in the sugarcane ash sample (6-7 % by number) than in the bagasse ash (~3 % by number). Moreover, the fibre-like particles in the sugarcane ash had a shorter diameter when compared with the bagasse ash samples.

FIGURE 1

Particle surface reactivity

Free radical production

None of the samples produced detectable $HO^{\bullet}$ or $CO_2^{\bullet-}$ radicals and, furthermore, addition of a reducing agent did not induce $CO_2^{\bullet-}$ release (results not reported for brevity). As a subsequent step, large amounts of $HO^{\bullet}$ were purposefully generated via the Fenton reaction in an aqueous solution, and the sample was added. In the presence of every ash sample, the signal of the DMPO-$HO^{\bullet}$ adducts was completely suppressed.

Bio-available Iron

During the 7 days of incubation all samples released iron into solution, measured as both removable Fe^{2+} (Fig. 2a) and total removable iron (Fig. 2b). The total amount of iron released from the samples was greater than that released from Min-U-Sil (a quartz standard with 0.075 % Fe_2O_3), which was shown to release 0.73 µmol m^{-2} over a period of 7 days (Horwell et al., 2007), but comparatively the samples released much lower amounts of iron than samples of volcanic ash previously tested in the same way. For example, Horwell et al., (2007) report a range of values for the total amount of iron released over a period of 7 days: 14 µmol m^{-2} from Merapi (Indonesia) ash to 655 µmol m^{-2} from Etna (Italy) ash. At the end of incubation the total iron released ranged between 2-3 µmol m^{-2}, for all samples, except for one of the sugarcane ash samples (A_ash1), which contains less than 1 µmol m^{-2} primarily in the oxidised (ferric, Fe^{3+}) form. Generally, the bagasse ash samples released more ferrous (Fe^{2+}) iron at the end of the experiment (~49 % of the total iron released after 7 days), which can readily participate in the Fenton reaction, when compared to the sugarcane ash samples (where ~12 % of the total iron released after 7 days was in the ferrous form) but, in general, the ferric iron was the dominant available form for all samples. In most cases, iron release was sustained during the first day of incubation and the kinetics of extraction progressively decreased with time.

FIGURE 2

Depletion of endogenous antioxidants

Statistical analysis (one-way ANOVA test) of the results revealed that none of the sugarcane or bagasse ash samples were significantly different from M120 negative control, and hence did not deplete (i.e. oxidise) the ascorbic acid to a greater extent than the known negative control. The effect of any transition metals on depletion of ascorbic acid was negligible, as indicated by the minimal difference between the +DTPA and –DTPA measured response of the ash samples (Fig. 3).

FIGURE 3

Surface hydrophilicity

Figure 4 shows the quantitative and energetic data relevant to the total and reversible adsorption of water vapour from the sugarcane ash (A_ash1) and bagasse ash (A_ashbag1). Both samples were hydrophilic. The total amount of water vapour adsorbed by the two samples was similar (Fig. 4a). At equilibrium pressure of 5 torr, sugarcane ash adsorbed ~4 μmol m^{-2} (0.6 μmol m^{-2} irreversibly, calculated as the difference between Adsorption I and II isotherms; Fig. 4a), while bagasse ash adsorbed ~3 μmol m^{-2} (1.1 μmol m^{-2} irreversibly). The extent of water vapour adsorbed is relatively low when compared to the heat released in the calorimetric isotherm (Fig. 4b). Water adsorption curves increased, for both the total and reversible adsorption, but with minor differences between the two samples. A_ash1 sugarcane trash ash irreversibly adsorbed a small amount of water vapour, at an equilibrium pressure >4 torr (Fig. 4a). Conversely, in A_ashbag1 bagasse ash the irreversible adsorption appeared at <0.8 torr and progressively increased with equilibrium pressure (Fig. 4a). A similar trend was observed for both A_ash1 and

A_ashbag1 calorimetric isotherms, but the difference between Adsorption I and II are less pronounced when compared to the volumetric isotherm for A_ashbag1 (Fig. 4b). The initial interaction energies were very high for both samples (~180 kJ mol^{-1}; Fig. 4c), which is greater than the latent enthalpy of liquefaction of water (44 kJ mol^{-1}). In both samples, the energy of interaction decreased until a plateau was reached for water coverage higher than 1 µmol m^{-2}.

FIGURE 4

Particle surface charge

Zeta potential of sugarcane (A_ash1) and bagasse ash (A_ashbag1) in solution at pH 7 was −40 and -30 mV respectively (Fig. 5), which indicates that the surface of particles in both samples have acidic character. No significant variation was observed in the magnitude of the zeta potential values of A_ashbag1 between pH 2 and 5, while the zeta potential of A_ash1 gradually decreased in the same range.

FIGURE 5

Cellular assays

Haemolysis

The erythrocyte lysis assay showed that the sugarcane and bagasse ash initiated a similar haemolytic response to the TiO_2 polymorph, which has a low (essentially negligible) haemolytic response (Fig. 6).

FIGURE 6

MH-S cellular response tests

A 24 hr incubation with the sugarcane ash sample (A_ash1) at high concentrations (80-120 µg cm^{-2}) induced a mild cytotoxic effect in the MH-S cells, measured as leakage of intracellular LDH activity into the extracellular medium (Fig. 7a). Conversely, the bagasse ash sample (A_ashbag1) did not significantly modify LDH release at any of the concentrations tested. A_ash1 was, however, significantly less cytotoxic than the positive control Min-U-Sil 5 at every concentration tested.

FIGURE 7

After 24 hr incubation with ash samples, the extracellular levels of nitrite were measured in the culture medium of MH-S cells. The accumulation of nitrite was significant only at the highest concentrations tested for both the sugarcane ash (A_ash1) and bagasse ash sample (A_ashbag1) (Fig. 7b). Again, Min-U-Sil 5 induced a significantly higher extracellular nitrite accumulation at all concentrations tested.

The levels of fluorescent compound DCF, formed as a result of the ROS generated by the samples or control, were measured after the 24 hr incubation period. The sugarcane ash samples (A_ash1) generated a greater concentration of ROS per mg of protein in the sample, when compared to the bagasse ash (A_ashbag1) (Fig. 7c). At the highest concentration A_ash1 and Min-U-Sil 5 generated a similar amount of ROS.

DISCUSSION

Particle surface area

The sugarcane and bagasse ash samples had a mean specific surface area of 55.8 $m^2\ g^{-1}$ and 59.0 $m^2\ g^{-1}$, respectively, in general agreement with Batra et al., (2008) who determined BET surface area values of 64 $m^2\ g^{-1}$ and 98 $m^2\ g^{-1}$ from two samples of bagasse ash collected from sugarcane estates in India.

Particle surface reactivity

Both sugarcane and bagasse ash samples contain small amounts of transition metal ions and crystalline silica (Le Blond et al., 2010; 2008). Nevertheless, no detectable hydroxyl or carbon centred radicals were formed after the addition of the ash to either H_2O_2 or sodium formate aqueous solutions. Conversely, Min-U-Sil quartz has previously been used as a positive control in other toxicity studies (e.g. measuring hydroxyl release from coal fly ash samples; van Maane et al., 1999) and has been shown to generate radical species under the same test conditions (e.g. Elias et al., 2006). Free radical production is also well documented for many toxic particulate samples containing transition metal ions, namely iron ions, e.g. asbestos minerals, such as crocidolite (e.g. Hardy and Aust, 1995; Kamp et al., 1992). Also volcanic ash generates substantial quantities of $HO^{\bullet}$ (Horwell et al., 2010; 2007; 2003) and, in some cases, a good correlation between iron ions available at the surface and Fenton activity has been observed.

One consideration is whether free radicals would form if the sample were fresh (i.e. analysed immediately after burning), or if the sample were ground. If covalent bonds are broken by mechanical failure (i.e. grinding), free radical species can arise on the new surface, formed by homolytic molecular cleavage. Fracture of crystalline silica, for instance, can produce highly reactive surface charges (e.g. Si^+ and SiO^-) or 'dangling bonds' (e.g. $^{\bullet}Si$ and $Si\text{-}O^{\bullet}$) (Fubini, 1998), which are not found on un-cleaved surfaces (Vallyathan et al., 1988; 1995). Further study

513 on samples of fresh and ground sugarcane ash would be useful to determine the extent to which
514 reactivity varies in aged/fresh or re-ground samples, as the ash is broken down by transportation
515 and the action of sugarcane cutters in the field.
516
517 All ash samples tested showed scavenging activity towards $HO^{\bullet}$, which is similar to the response
518 observed when engineered carbon-based materials such as carbon black (Mwila et al., 1994),
519 multi-walled carbon nanotubes (MWCNT) (Fenoglio et al., 2006) and fullerenes (Morton et al.,
520 1992; Krusic et al., 1991) have been tested. The implications at the biological level of this type of
521 scavenging activity are, however, still unclear. No experimental data currently exist on the
522 potential scavenging activity of other carbonbased particulates, e.g. coal dusts from mines, but
523 epidemiological studies on mine-workers have shown that the biological effects of quartz-
524 containing coal dust include simple pneumoconiosis, emphysema and accelerated loss of lung
525 function (IARC 1997). Coal dusts have not been classified as carcinogenic to humans.
526 Furthermore, some studies have shown that quartz has less biological activity when it is ground
527 with coal mine dust (Le Bouffant et al., 1982; Martin et al., 1972; Ross et al., 1962). Further
528 investigations are needed to establish if coal dusts may also show scavenging activity and if this
529 activity may be responsible for their low toxicity.
530
531
532 A small amount of iron ions, mainly in the oxidized form, was available on the particle surfaces
533 of all samples examined. No obvious difference was observed between bagasse and sugarcane ash
534 samples, except an elevated amount of ferrous ions on the bagasse surface when compared with
535 the sugarcane surface. However, these ions are not able to induce the Fenton reaction.
536
537 Both the sugarcane ash and bagasse ash samples are hydrophilic, as the energies of interaction
538 between the water and particle surface were very high. Hydrophilic surfaces favour cell surface

539 adhesion, protein absorption and denaturation, which can lead to injury (Fubini and Otero Areán,
540 1999; Fubini et al., 1998; Donaldson et al., 1993). The amount of water molecules adsorbed at the
541 samples' surfaces was low when compared with quartz or other crystalline silica types and high in
542 comparison to carbonaceous materials such carbon nanotubes (Fenoglio et al., 2008). In the case
543 of crystalline silica, the presence of silanols makes the surface more hydrophilic, while the
544 absence of oxygenated groups makes pristine carbon nanotubes (CNT) hydrophobic. Heating the
545 silica surface may reduce the hydrophilicity because of the transformation of silanols into
546 siloxanes (Fubini et al., 1995b; Pandurangi et al., 1990). Oxidising coals and other carbonaceous
547 material increases the hydrophilicity of the surface, while heating in reduced or inert conditions
548 will render the surface more hydrophobic (Groszek and Partyka, 1993), which has been
549 demonstrated both in graphites and carbon black (Groszek, 1987). Although the sugarcane ash
550 products have been heated during combustion the samples still display hydrophilicity with high
551 energies of interactions with water vapour. These energies of interaction may be due to the
552 presence of transition metals or alkaline metal ions on the sample surfaces that have a high
553 affinity to water molecules and are distributed on a low hydrophilic surface (on carbon patches
554 for example). The trend of the volumetric and calorimetric curves also suggests that dissociative
555 adsorption takes place upon the earliest contact with water vapour.
556
557 The zeta potential measurements of the sugarcane and bagasse ash samples, showed that the
558 surfaces are negatively charged (measured between pH 2-8). Oxygenated groups (e.g. carboxylic
559 and phenolic groups, usually present on carbon surfaces, and silanol groups on the silica
560 frameworks) were likely responsible for the shift to the more negative charge. Carboxylic groups
561 with PKa values between 2.0 and 5.0 could account for the hydrolysed fraction, and phenolic
562 groups for the non-hydrolysed fraction of the carbon surfaces. The differences in the trend of the
563 zeta potential curves as a function of pH could be related to the different acidity of the surface

functional groups (Lau et al., 1986) and that suggests the presence of weak-acid functional groups (Pka=4.5) on the bagasse ash and acidic groups (Pka=2) on the sugarcane ash samples.

Surface groups able to establish hydrogen bonds and negative charge sites able to interact with organic cations, e.g. with quaternary ammonium ions of erythrocytes, may affect the haemolytic potential. The hydrophilicity and negative surface charges displayed by the samples at physiologically-relevant pH could explain the behaviours observed in the haemolysis assay.

Cellular assays

The samples of sugarcane and bagasse ash tested here did not oxidise ascorbic acid. The presence of DTPA (chelating agent) was only shown to inhibit the oxidation of ascorbic acid by ROFA, and the London control particulate samples. Both the ROFA and London control samples are, thus, likely to have transition metals on the particles' surfaces. The same response was not observed for sugarcane or bagasse ash, which would indicate that, in this case, transition metals are not involved in any ascorbic acid depletion.

The haemolysis assay can be used to investigate the particle membranolytic activity and provides a simple and rapid approach to studying the effects of particles on biological membranes. However, the exact mechanism of the haemolytic activity is still unclear. The sugarcane ash and bagasse ash samples did not show any significant haemolytic activity above that observed for TiO_2 (known negative control) when incubated with erythrocytes for 20 min. Conversely, DQ12 quartz induced a markedly greater response when compared to the samples. DQ12 is a highly hydrophilic quartz (Fubini et al., 1995). Surface silanols are widely dissociated at physiological pH as indicated by its negative zeta potential (Ghiazza et al., 2011). The difference in the activity in haemolytic tests between ash and DQ12 could thus be related to the different extent of the disassociated silanols' and anionic sites' capacity to interact with cell membranes. Murashov et

al., (2006) showed a direct correlation between silanol densities found on silica frameworks (namely tridymite, quartz and cristobalite), in appropriate positions (i.e. geminal silanols), and the samples' haemolytic activity.

No LDH release from alveolar macrophages was found at low concentrations. The sugarcane ash stimulated a cytotoxic response at higher concentrations, while the bagasse ash did not appear to induce a similar reaction until the very highest concentrations were tested. However, the cytotoxic response, in the form of NO production, for both the sugarcane and bagasse ash samples was significantly lower than that of the Min-U-Sil 5 positive control. Only ROS generation by the sugarcane ash samples was significantly different at the higher concentration. In this case, the scavenging activity observed in the cell free test could not be sufficient to neutralize all ROS produced by cells, during 24 hr incubation.

CONCLUSIONS

Particle size and morphology, surface properties commonly implied in the biological response, haemolytic, cytotoxic activity and ability to induce oxidative stress have been investigated to elucidate the potential toxicity of ash produced during commercial sugarcane harvesting and processes during sugar production.

The sugarcane and bagasse ash do not show most of the chemico-physical properties typical of toxic particulate: the ash samples tested here do not readily produce hydroxyl or carbon-centred free radicals or release substantial quantities of iron that could subsequently drive free-radical production. The low surface reactivity is likely related to the particular chemical composition of ash samples, with minor crystalline silica and iron phases perhaps being partially covered by a more inert carbon layer. The ash samples do, however, have the capacity to scavenge free radicals in an external solution of hydroxyl radicals produced by the Fenton reaction. Although a correlation has been observed between free radical scavenging and an inflammatory response (for example) in some particulate samples (e.g. multi-walled carbon nanotubes), the precise implications of this feature are still unclear (Fenoglio et al., 2008). The sample surfaces of both the sugarcane ash and bagasse ash tested were hydrophilic, which could indicate that the particles could interact with biological molecules. The degree of hydrophilicity is low, however, when compared to crystalline silica. Zeta potential, measured at a variety of pH levels, shows that the particle surfaces are negatively charged, which may, again, mean that they could potentially interact with organic cations of the biological membranes. Despite these surface properties the samples did not display haemolytic activity. The samples did not oxidise ascorbic acid, which simulates the effects of particulate matter on the lung lining fluid and the potential to trigger acute respiratory symptoms, such as asthma. In the cellular tests, the samples induced reactive oxygen species and reactive nitrogen species, which are associated with both cytotoxic and mutagenic

effects, only at the highest concentrations tested. However, the magnitudes of these reactions were significantly lower than the crystalline quartz used as a positive control.

FUNDING SOURCES

JSL's work was supported by a NERC CASE studentship (Grant No. NER/S/A/2006/14107) with the University of Cambridge and the Natural History Museum, London. CJH acknowledges a NERC Postdoctoral Research Fellowship (Grant No. NE/C518081/2).

REFERENCES

Amre DK, Infante-Rivard C, Dufresne A, Durgawale PM, Ernst P. 1999. Case-control study of lung cancer among sugar cane farmers in India. Occup Environ Med 56(8):48-552.

Arbex MA, Martins LC, Oliveira RC, Pereira LAA, Arbex FF, Cançado JED, Saldiva PHN, Braga ALF. 2007. Air pollution from biomass burning and asthma hospital admissions in a sugar cane plantation area in Brazil. J Epidemiol Commun H 61:395-400.

Arbex MA, Böhm GM, Saldiva PHN, Conceição GMS, Pope CA III, Braga ALF. 2000. Assessment of the effects of sugar cane plantation burning on daily counts of inhalation therapy. J Air Waste Manage 50:1745-1749.

Ayres JG, Borm P, Cassee FR, Castranova V, Donaldson K, Ghio A, Harrison RM, Hider R, Kelly F, Kooter IM, Marano F, Maynard RL, Mudway I, Nel A, Sioutas C, Smith S, Baeza-Squiban A, Cho A, Duggan S, Froines J. 2008. Evaluating the toxicity of airborne particulate matter and nanoparticles by measuring oxidative stress potential - A workshop report and consensus agreement. Inhal Toxicol 20:75-99.

Baker WS, Long JW, Stroud RM, Rolison DR. 2004. Sulfur-functionalized carbon aerogels: a new approach for loading high-surface-area electrode nanoarchitectures with precious metal catalysts. J Non-Cryst Solids 350:80-87.

Batra VS, Urbonaite S, Svensson G. 2008. Characterisation of unburned carbon in bagasse fly ash. Fuel 87:2972-2976.

Bolis V, Fubini B, Coluccia S, Mostacci E. 1985. Surface hydration of crystalline and amorphous silicas. J Therm Anal 30:1283-1292.

Boopathy R, Asrabadi BR, Ferguson TG. 2002. Sugar cane (Saccharum offcinarum) burning and asthma in southeast Louisiana, USA. Bull Environ Contam Toxicol 68(2):173-179.

Cançado JED, Saldiva PHN, Pereira LAA, Lara LBLS, Artaxo P, Martinelli LA, Arbex MA, Zanobetti, Braga ALF. 2006. The impact of sugar cane burning emissions on the respiratory system of children and the elderly. Environ Health Persp 114(5):725-729.

Clouter A, Brown D, Höhr D, Borm P, Donaldson K. 2001. Inflammatory effects of respirable quartz collected in workplaces versus standard DQ12 quartz: Particle surface correlates. Toxicol Sci 63:90-98.

Dalal NS, Shi X, Vallyathan V. 1990. ESR spin trapping and cytotoxicity investigations of freshly fractured quartz: mechanism of acute silicosis. Free Radical Res Com 9:259-266.

Donaldson K, Miller BG, Sara E, Slight J, Brown C. 1993 Asbestos fibre length-dependent detachment injury to alveolar epithelial cells in vitro: role of a fibronectin-binding reception. Int J Exp Pathol 74:243-250.

Elias Z, Poirot O, Fenoglio I, Ghiazza M, Danière M- C, Terzetti F, Darne C, Coulais C, Matesovits I, Fubini B. 2006. Surface reactivity, cytotoxic, and morphological transforming effects of diatomaceous earth products in Syrian Hamster embryo cells. Tox Sci 92(2):510-520.

Fenoglio I, Greco G, Tomatis M, Muller J, Raymundo-Piñero E, Béguin F, Fonseca A, Nagy J, Lison D, Fubini B. 2008. Structural defects play a major role in the acute lung toxicity of multiwall carbon nanotubes: Physicochemical aspects. Chem Res Toxicol 21:1690-1697.

Fenoglio I, Tomatis M, Lison D, Muller J, Fonsa A, Nagy JB, Fubini B. 2006. Reactivity of carbon nanotubes: Free radical generation or scavenging activity? Free Radical Bio Med 40:1227-1233.

Fubini B, Hubbard A. 2003. Reactive oxygen species (ROS) and reactive nitrogen species (RNS) generation by silica in inflammations and fibrosis. Free Radical Bio Med 34:1507-1516.

Fubini B, Otero-Aréán C. 1999. Chemical aspects of the toxicity of inhaled mineral dusts. Chem Soc Rev 28:373-381.

Fubini B, Aust AE, Bolton RE, Borm PJA, Bruch J, Ciapetti G, Donaldson K, Elias Z, Gold MC, Jaurand C, Kane AB, Lison D, Muhle H. 1998. Non-animal tests for evaluating the toxicity of solid xenobiotics. ATLA 26:579-617.

690 Fubini B. 1998. Health Effects of Silica. In: Legrand AP. The Surface Properties of Silicas. John
691 Wiley and Sons, Ltd. p 415-464.
692 Fubini B, Mollo L, Giamello E. 1995. Free radical generation at the solid/liquid interface in iron
693 containing minerals. Free Rad Res 23:593-614.
694 Fubini B, Bolis V, Cavenago A, Volante M. 1995b. Physiochemical properties of crystalline
695 silica dusts and their possible implication in various biological responses. Scand J Work
696 Environ Health 21:9-14.
697 Fubini B, Giamello E, Volante M, Bolis V. 1990. Chemical functionalities at the silica surface
698 determining its reactivity when inhaled. Formation and reactivity of surface radicals.
699 Toxicol Ind Health 6(6):571-598.
700 Fubini B, Giamello E, Pugliese L, Volante M. 1989. Mechanically induced defects in quartz and
701 their impact on pathogenicity. Solid State Ionics 32-33:334-343.
702 Fubini B, Bolis V, Giamello E. 1985. Description of surface structures by adsorption
703 microcalorimetry. Thermochim Acta 85:23-26.
704 Ghigo D, Aldieri E, Todde R, Costamagna C, Garbarino G, Pescarmona G, Bosia A. 1998.
705 Chloroquine stimulates nitric oxide synthesis in murine, porcine, and human endothelial
706 cells. J Clin Invest 102:595–605.
707 Giamello E, Fubini B, Volante M, Costa D. 1990. Surface oxygen radicals originating via redox
708 reactions during the mechanical activation of crystalline SiO_2 in hydrogen peroxide.
709 Colloid Surface 45:155-165.
710 Godri KJ, Duggan ST, Fuller GW, Baker T, Green D, Kelly FJ, Mudway IS. 2010. Particulate
711 matter oxidative potential from waste transfer station activity. Environ. Health Persp
712 118(4):493-498.
713 Greg SJ, Sing KSW. 1982. Adsorption, surface area and porosity (second edition). London:
714 Academic Press.

715 Groszek AJ, Partyka S. 1993. Measurement of hydrophobic and hydrophilic surface sites by flow
716 microcalorimetry. Langmuir 9:2721-2725.
717 Groszek AJ. 1987. Graphitic and polar surface sites in carbonaceous solids. Carbon 25:717-722.
718 Hardy JA, Aust AE. 1995. Iron in asbestos chemistry and carcinogenicity. Chem Rev 95:97-118.
719 Horwell CJ, Stannett GW, Andronico D, Bertagnini A, Fenoglio I, Fubini B, Le Blond JS,
720 Williamson BJ. 2010. A physico-chemical assessment of the health hazard of Mt.
721 Vesuvius volcanic ash. J Volcanol Geotherm Res 191:222-232.
722 Horwell CJ, Fenoglio I, Fubini B. 2007. Iron-induced hydroxyl radical generation from basaltic
723 volcanic ash. Earth Planet Sci Lett 261:662-669.
724 IARC (International Agency for Research on Cancer). 1997. Silica, some silicates, coal dust and
725 para-aramid fibrils. In: IARC Monographs on the Evaluation of Carcinogenic Risks to
726 Humans (vol. 68). Lyon, France, pp. 40.
727 Jaurand M-C. 1997. Mechanisms of fibre-induced genotoxicity. Environ Health Persp 105(Suppl.
728 5):1073-1084.
729 Kamp DW, Graceffa P, Pryor WA, Weitzman SA. 1992. The role of free-radicals in asbestos
730 induced diseases. Free Radical Biol Med 12:293-315.
731 Kelly FJ. 2003. Oxidative stress: Its role in air pollution and adverse health effects. Occup
732 Environ Med 60:612-616.
733 Kelly FJ, Mudway I, Blomberg A, Frew AJ, Sanström T. 1999. Altered lung antioxidant status in
734 patients with mild asthma. Lancet 354:482-483.
735 Krusic PJ, Wasserman E, Keizer PN, Morton JR, Preston KF. 1991. Radical reaction of C60.
736 Science 254:1183-1185.
737 Lau AC, Furlong DN, Healy TW, Grieser F. 1986. The electrokinetic properties of carbon black
738 and graphitized carbon black aqueous colloids. Colloid Surface 18(1):93-104.
739 Le Blond JS, Horwell CJ, Williamson BJ, Oppenheimer C. 2010. Generation of crystalline silica
740 from sugarcane burning. J Environ Monitor *12*:1459-1470.

741 Le Blond JS, Williamson BJ, Horwell CJ, Monro AK, Kirk CA, Oppenheimer C. 2008.
742 Production of potentially hazardous respirable silica airborne particulate from the burning
743 of sugarcane. Atmos Environ 42:5558-5568.
744 Le Bouffant L, Daniel H, Martin JC, Bruyere S. 1982. Effect of impurities and associated
745 minerals on quartz toxicity. Ann Occup Hyg 26:625–634.
746 Li N, Hao M, Phalen RF, Hinds W, Nel E. 2003. Particulate air pollutants and asthma: a paradigm
747 for the role of oxidative stress in PM-induced adverse health effects. Cl Immunol 3:250-
748 265.
749 Light WG, Wei ET. 1977. Surface charge and hemolytic activity of asbestos. Environ Res
750 13(1):135-145.
751 Lopes FS, Ribeiro H. 2006. Mapeamento de internações hospitalares por problemas respiratórios
752 e possíveis associações à exposição humana aos produtos da quiema da palha de cana-de-
753 açúcar no estado de São Paulo. Rev Bras Epidemiol 9(2):215-225.
754 Martin JC, Daniel-Moussard H, Le Bouffant L, Policard, A. 1972. The role of quartz in the
755 development of coal workers' pneumoconiosis. Ann N Y Acad Sci 200:127-141
756 Mazzoli-Rocha F, Bichara Magalhaes C, Malm O, Hilario Nascimento Saldiva P, Araujo Zin W,
757 Faffe DS. 2008. Comparative respiratory toxicity of particles produced by traffic and
758 sugar cane burning. Environ Res 108(1):35-41.
759 Miller CR, Bondurant B, McLean SD, McGovern KA, O'Brien DF. 1998. Liposome−cell
760 interactions in vitro: effect of liposome surface charge on the binding and endocytosis of
761 conventional and sterically stabilized liposomes. Biochem 37(37):12875-12883
762 Morton JR, Preston KF, Krusic PJ, Hill A, Wasserman E. 1992. ESR studies of the reaction of
763 alkyl radicals with C-60. J Phys Chem 96:3576-3578.
764 Murashov V, Harper M, Demchuk D. 2006. Impact of silanol surface density on the toxicity of
765 silica aerosols measured by erythrocyte haemolysis. J Occup Environ Hyg 3:718–723.

766 Mwila J, Miraftab M, Horrocks AR. 1994. Effect of carbon black on the oxidation of
767 polyolefins—An overview. Polym Degrad Stab 44(3):351-356
768 Pandurangi RS, Seera MS, Razzaboni BL, Bolsaitis P. 1990. Surface and bulk infrared modes of
769 crystalline and amorphous silica particles: a study on the relation of surface structure to
770 cytotoxicity of respirable silica. Environ Health Persp 86:327-336.
771 Park S-H, Aust AE. 1998. Participation of iron and nitric oxide in the mutagenicity of asbestos in
772 hgprt2, gpt1 chinese hamster V79 cells. Cancer Res 58:1144–1148.
773 Polimeni M, Gazzano E, Ghiazza M, Fenoglio I, Bosia A, Fubini B, Ghigo D. 2008. Quartz
774 inhibits glucose 6-phosphate dehydrogenase in murine alveolar macrophages. Chem Res
775 Toxicol 21(4):888-894.
776 Pope III, CA. 2000. Epidemiology of fine particulate air pollution and human health: Biologic
777 mechanisms and who's at risk? Environ Health Persp 108(4):713-723.
778 Ribeiro R. 2009. Sugar cane burning in Brazil: respiratory health effects. Rev Saúde Pública
779 42(2):1-6.
780 Ross HF, King EJ, Yoganathan M, Nagelschmidt G. 1962. Inhalation experiments with coal dust
781 containing 5 percent, 10 percent, 20 percent and 40 percent quartz: tissue reactions in the
782 lungs of rats. Ann Occup Hyg 5;149-161.
783 Schmidt HHHW, Walter U. 1994. NO at work. Cell 78:919–925.
784 Schoonen MAA, Chn CA, Roemer E, Laffers R, Simon SR, O'Riordan T. 2006. Mineral-induced
785 formation of reactive oxygen species. Rev Mineral Geochem 64(1):179-221.
786 Shi X, Mao Y, Daniel LN, Saffiotti U, Dalal NS, Vallyathan V. 1995. Generation of reactive
787 oxygen species by quartz particles and its implication for cellular damage. Appl Occup
788 Environ Hyg 10:1138-1144.
789 Sing KSW, Everett DH, Haul RAW, Mouscou L, Pierotti RA, Roquérol J, Siemieniewska T.
790 1985. Reporting physisorption data for the gas/solid systems with special reference to the
791 determination of surface area and porosity. Pure & Appl Chem 57:603-619.

792 Vallyathan V, Castranova V, Pack D, Leonard S, Shumaker J, Hubbs AF, Shoemaker DA,
793 Ramsey DM, Pretty JR, McLaurin JL, Khan A, Teass A. 1995. Freshly fractured quartz
794 inhalation leads to enhanced lung injury and inflammation: Potential role of free radicals.
795 Am J Resp Crit Care 152(3):1003-1009.
796 Vallyathan V, Shi X, Dalal NS, Irr W, Castranova V. 1988. Generation of free radicals from
797 freshly fractured silica dust: potential role in acute silica-induced lung injury. Am Rev
798 Respir Dis 138:1213-1219.
799 Van Oss CJ. 1994. Interfacial forces in aqueous media. New York: Marcel Dekker, p 308-332
800 Wink DA, Mitchell JB. 1998. Chemical biology of nitric oxide: insights into regulatory, cytotoxic
801 and cytoprotective mechanisms of nitric oxide. Free Radic Biol Med 25:434–456.
802

TABLE AND FIGURE CAPTIONS

Table 1 Sample collection and treatment details (from Le Blond et al., 2010).

Table 2 Summary of the methods used to analyse sugarcane and bagasse ash samples.

Table 3 Particle size and specific surface area data for the samples of sugarcane and bagasse ash.

Figure 1 The aspect ratio and major axis diameter of the a) sugarcane ash (A_ash1) b) bagasse ash (A_ashbag1), and selected images of fibre-like particle morphology in c) A_ash1 and d) A_ashbag1. The intensity of the grey denotes the concentration of data plotted onto the scattergram.

Figure 2 Removable Fe in samples of sugarcane ash (A_ash1 and B_ash7) and bagasse ash (A_ashbag1 and A_ashbag2), shown as a) Fe^{2+} release (with ferrozine solution) and b) total (Fe^{2+} + Fe^{3+} release, with ferrozine solution plus ascorbic acid as a reducing agent). Measurements were in duplicate and presented as averages $\pm$ standard deviation.

Figure 3 Measured ascorbic acid depletion after incubation with the sugarcane and bagasse ash samples, including the control (CONT), internal standards (M120: negative control, ROFA: positive control, LEZ B11-14 and LEZ B11-20: airborne particulate samples collected in London, with a medium and low known oxidation response, respectively) and standard deviations for each measurement. All samples and controls are run both in the presence (+) and absence (-) of a chelating agent (DTPA). Measurements were in triplicate and presented as averages $\pm$standard deviation.

Figure 4 Micro-calorimetry data for sugarcane ash sample A_ash1 and bagasse ash A_ashbag1 a) volumetric isotherm (amount of water adsorbed), b) calorimetric isotherm (total heat released), and c) interaction energy of water molecules vs. amount of water adsorbed (1 torr = 133.322 Pa).

Figure 5 Zeta potential as function of pH. Measurements were in triplicate and presented as averages ± standard deviation.

Figure 6 Haemolysis reactions from incubation with the sugarcane and bagasse ash samples, including TiO_2 (negative control) and DQ12 (positive control). Measurements were in triplicate and presented as averages ±standard deviation.

Figure 7 MH-S cellular responses by measuring the following, in the presence of sugarcane ash sample A_ash1, bagasse ash sample A_ashbag1 or Min-U-Sil 5 (positive control), at concentrations of 0, 20, 40, 80, 120 µg cm^{-2}, a) LDH release, calculated as percentage of total LDH activity (n=5), b) extracellular levels of nitrite (n=5), and c) intracellular ROS production (n=4). All measurements were performed in duplicate and presented as averages ± standard error vs. ctrl: * $p<0.01$, ** $p<0.001$, *** $p<0.0001$, ^ $p<0.005$.

1 **TABLES**

2 **Table 1**

Sample type	Sample name	Collection details	Post-collection treatment
Sugarcane ash	Country(A/B)_ ash#	Sampled from the top 4 cm of the accumulated ash (taking care not to disturb/include the underlying soil), at 12 randomly chosen sites within each of the 7 plots, immediately after the pre-harvest burn.	Samples were homogenised (within each plot).
Bagasse ash	A_ashbag#	Collected directly from the water flushed out from bagasse-burning boilers (periodically flushed out to clear the residual ash). A_ashbag1: supernatant liquid portion of the water. A_ashbag2: sediment in settlement ponds.	The ash-water mixture was desiccated in an oven (60 $^{\circ}$C for 7 days) and homogenised (within each collection)

3 **Table 2**

Sample	Particle surface properties	Toxicity assays

	Particle size and surface area	Particle shape	HO· and $CO_2^{\cdot-}$ production and HO· scavenging	Available Fe	Surface charge	Surface hydrophilicity/ hydrophobicity	Depletion of antioxidant defences	Haemolysis	MH-S cellular responses
A_ash1	√	√	√	√	√	√	√	√	√
A_ash2	√						√	√	
A_ash3	√						√	√	
A_ash4	√						√	√	
A_ash5	√						√	√	
B_ash6	√						√	√	
B_ash7	√		√	√			√	√	
A_ashbag1	√	√	√	√	√	√	√	√	√
A_ashbag2	√		√	√			√	√	

Table 3

Sample	Mean particle diameter (μm)	Surface area (m^2 g^{-1})[a]	BET error (m^2 g^{-1})[a]
A_ash1	78.8	87.2[b]	4.2[b]
A_ash2	101.6[1]	18.6	0.3
A_ash3	96.0	89.9[b]	2.8[b]
A_ash4	95.2	87.8[b]	3.70
A_ash5	84.1	70.1[b]	2.3[b]
B_ash6	76.8	21.2[b]	0.3[b]
B_ash7	162.0	16.1	0.2
A_ashbag1	46.1	62.6[b]	2.3[b]
A_ashbag2	176.0	55.4[b]	0.5[b]

[a] average from 3 repeats.

[1] [b]Langmuir surface area (monolayer adsorption).

Figure 1

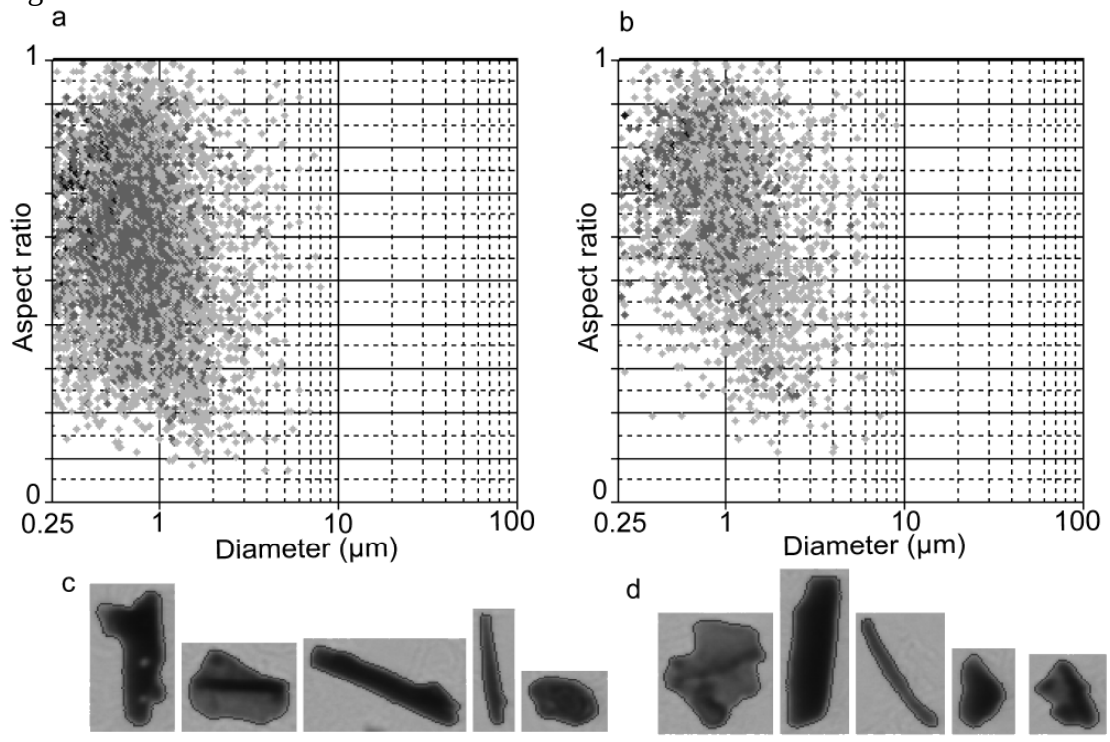

Figure 2

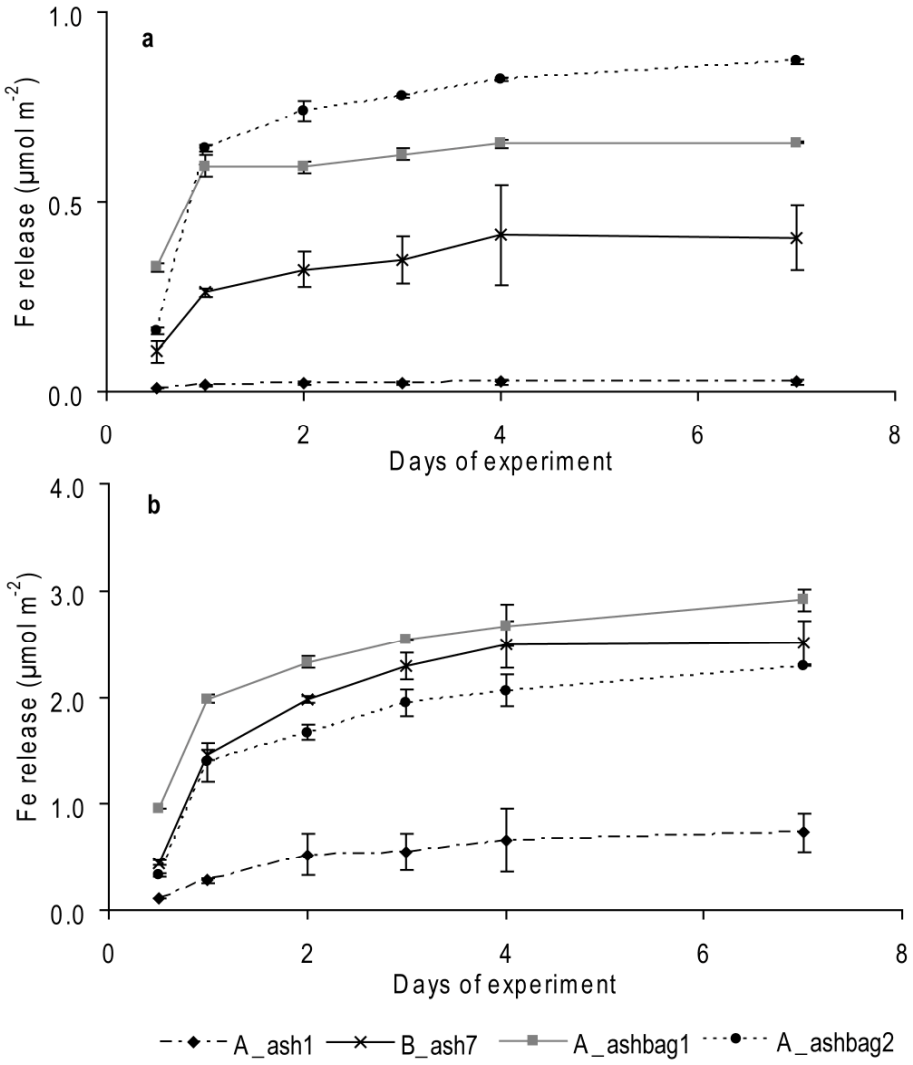
a
b
Fe release (µmol m-2)
Days of experiment
A_ash1
B_ash7
A_ashbag1
A_ashbag2

Figure 3

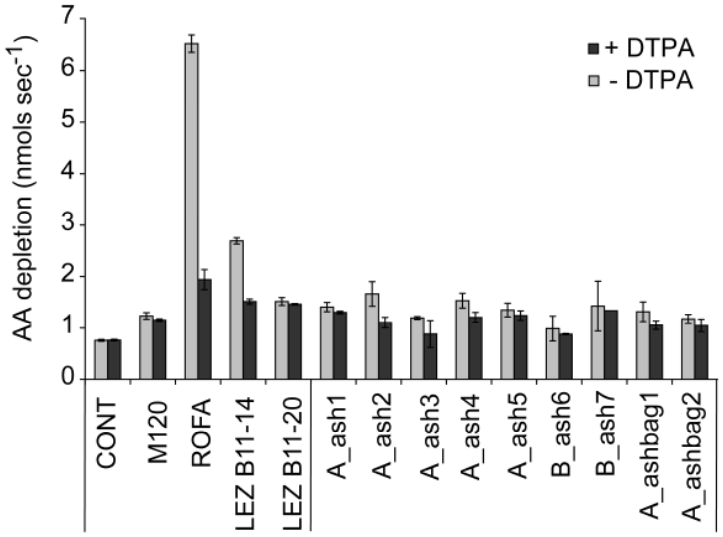
AA depletion (nmols sec-1)
7
6
5
4
3
2
1
0
+ DTPA
- DTPA
CONT
M120
ROFA
LEZ B11-14
LEZ B11-20
A_ash1
A_ash2
A_ash3
A_ash4
A_ash5
B_ash6
B_ash7
A_ashbag1
A_ashbag2

Figure 4

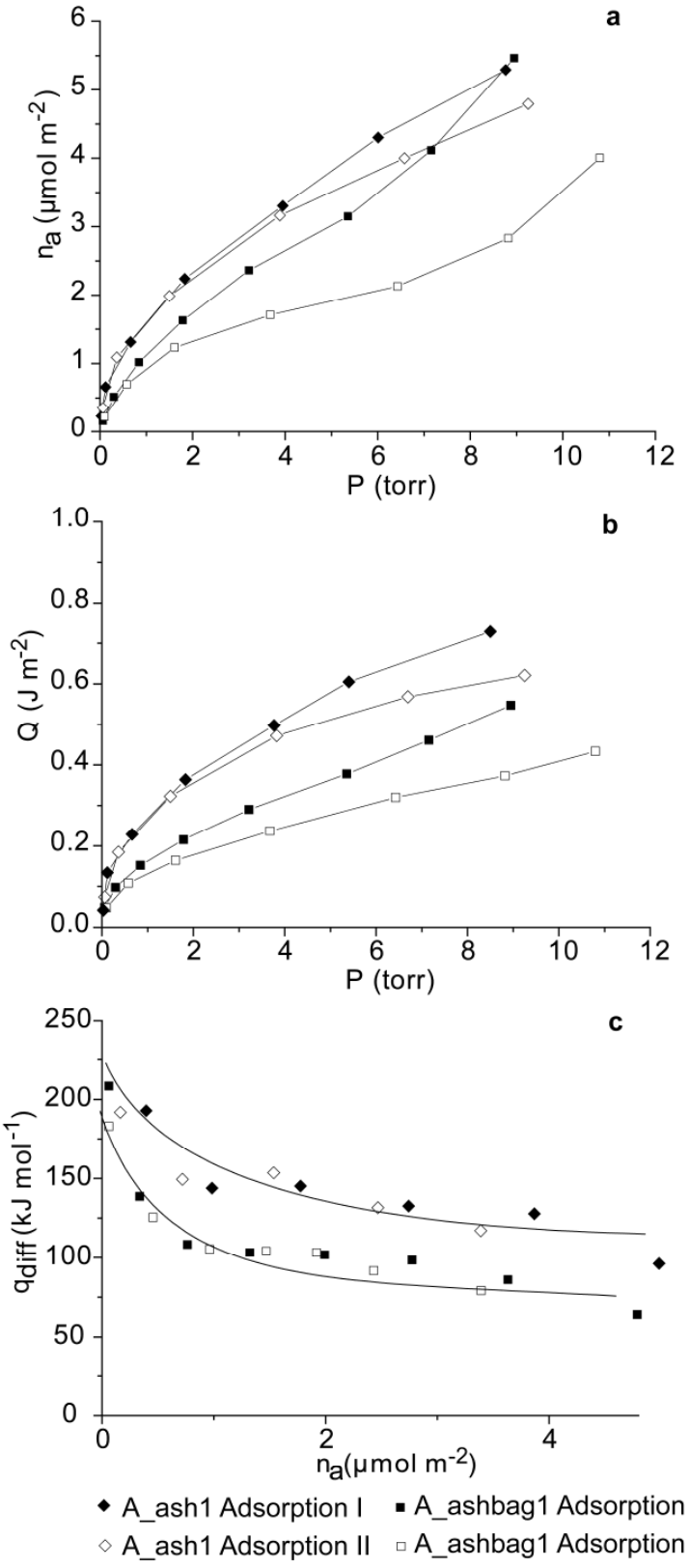
a
n_a (µmol m^{-2})
P (torr)
b
Q (J m^{-2})
P (torr)
c
q_{diff} (kJ mol^{-1})
n_a(µmol m^{-2})
A_ash1 Adsorption I
A_ashbag1 Adsorption
A_ash1 Adsorption II
A_ashbag1 Adsorption

Figure 5

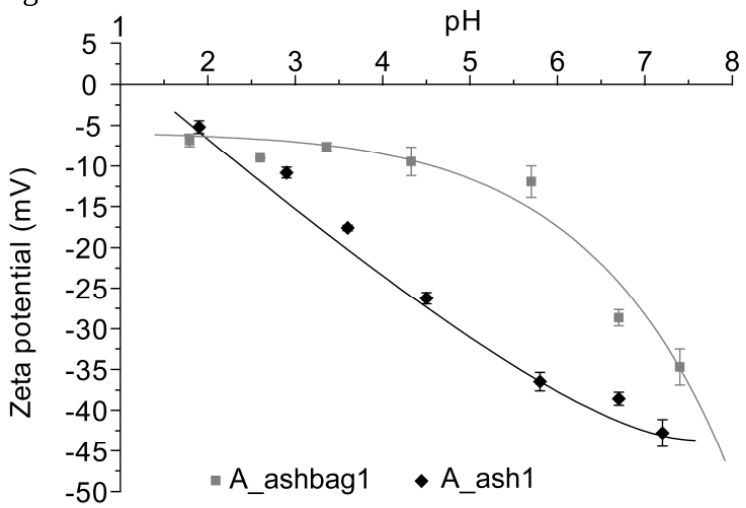
pH
1
2
3
4
5
6
7
8
5
0
-5
-10
-15
-20
-25
-30
-35
-40
-45
-50
Zeta potential (mV)
A_ashbag1
A_ash1

Figure 6

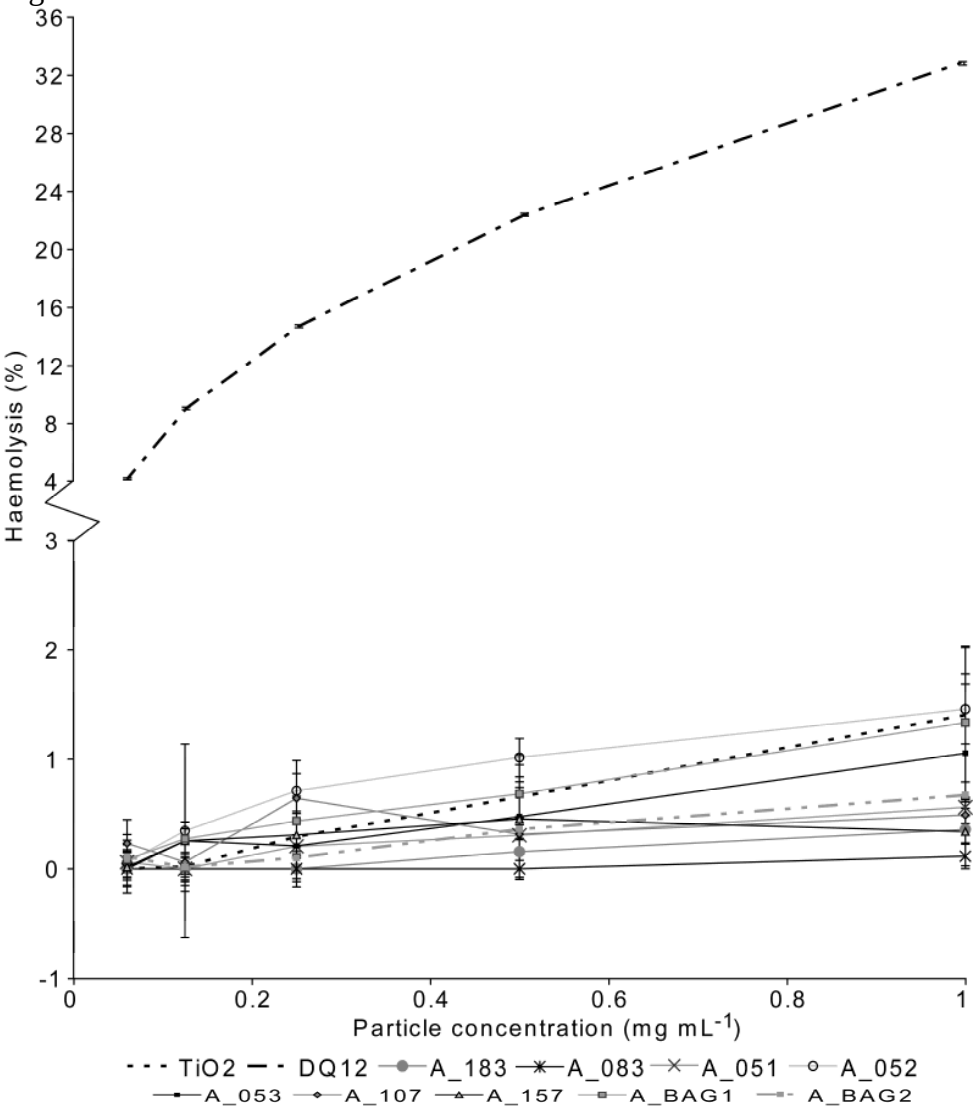
Haemolysis (%)
36
32
28
24
20
16
12
8
4
3
2
1
0
-1
0
0.2
0.4
0.6
0.8
1
Particle concentration (mg mL-1)
TiO2
DQ12
A_183
A_083
A_051
A_052
A_053
A_107
A_157
A_BAG1
A_BAG2

Figure 7

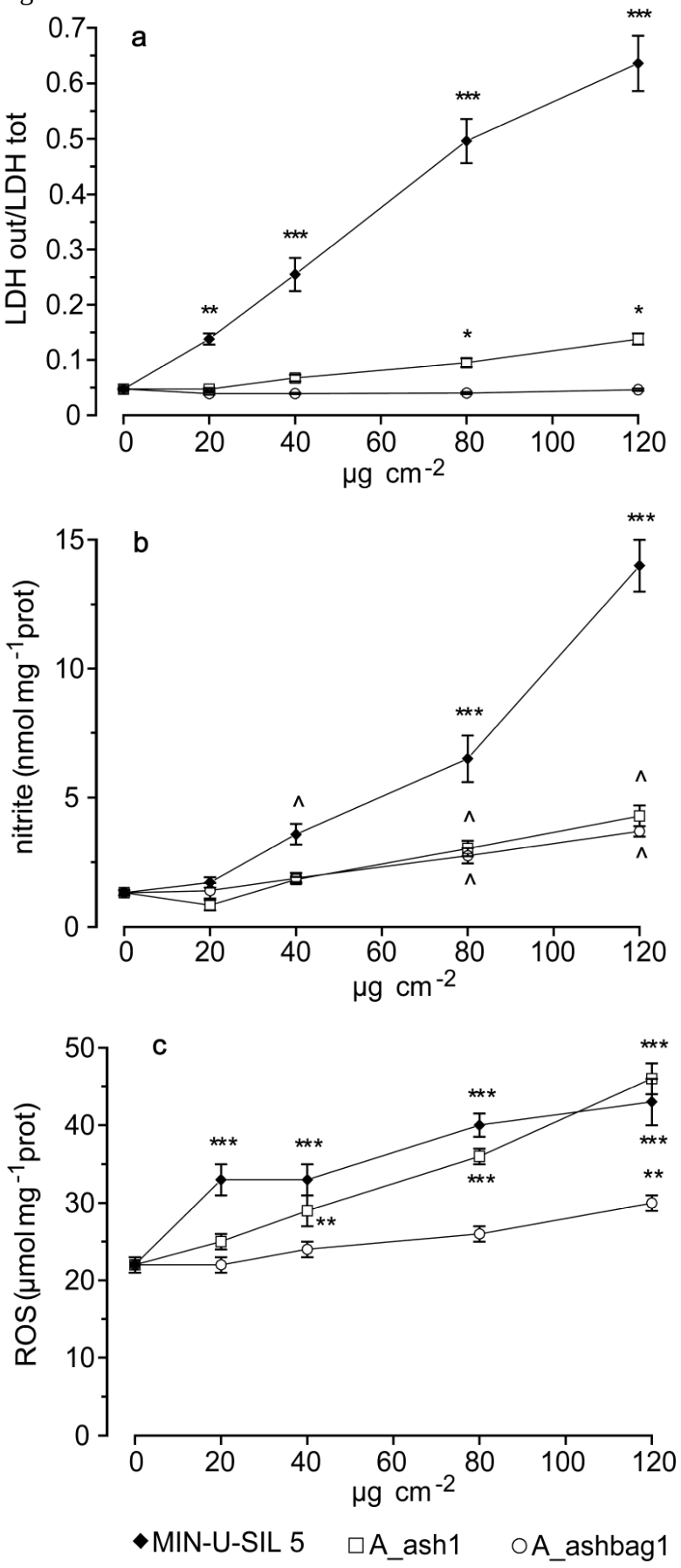
a
LDH out/LDH tot
0.7
0.6
0.5
0.4
0.3
0.2
0.1
0
0
20
40
60
80
100
120
µg cm-2
**
***
***
*
*
***
b
nitrite (nmol mg-1prot)
15
10
5
0
^
^
^
^
^
***
***
c
ROS (µmol mg-1prot)
50
40
30
20
10
0
***
***
***
***
**
***
**
MIN-U-SIL 5
A_ash1
A_ashbag1